An Updated Optical Design for the Off-Plane Grating Rocket Experiment

Benjamin D. Donovan[a], Randall L. McEntaffer[a], James H. Tutt[a], Bridget C. O'Meara[a], Fabien Grisé[a], Kim A. Allgood[b,c], Michael P. Biskach[b,c], Kai-Wing Chan[b,d], Michal Hlinka[b,c], John D. Kearney[b,c], James R. Mazzarella[b,c], Ryan S. McClelland[b,c], Ai Numata[b,c], Raul E. Riveros[b,d], Timo T. Saha[b], Peter M. Solly[b,c], William W. Zhang[b], Andrew D. Holland[e], Matthew R. Lewis[e], Matthew R. Soman[e], and Karen Holland[f]

[a]The Pennsylvania State University, University Park, PA 16802
[b]NASA Goddard Space Flight Center, Greenbelt, MD 20771
[c]KBRwyle Space Engineering Division, Greenbelt, MD 20770
[d]University of Maryland-Baltimore County, Baltimore, MD 21250
[e]The Open University, Walton Hall, Milton Keynes, UK
[f]XCAM Ltd., Northampton, UK

ABSTRACT

The Off-plane Grating Rocket Experiment (OGRE) is a soft X-ray spectroscopy suborbital rocket payload designed to obtain the highest-resolution soft X-ray spectrum of Capella to date. With a spectral resolution goal of $R(\lambda/\Delta\lambda) > 2000$ at select wavelengths in its 10-55 Å bandpass of interest, the payload will be able to study the line-dominated spectrum of Capella in unprecedented detail. To achieve this performance goal, the payload will employ three key technologies: mono-crystalline silicon X-ray mirrors developed at NASA Goddard Space Flight Center, reflection gratings manufactured at The Pennsylvania State University, and electron-multiplying CCDs developed by The Open University and XCAM Ltd. In this document, an updated optical design that can achieve the performance goal of the OGRE spectrometer and a new grating alignment concept to realize this optical design are described.

Keywords: optical design, soft X-ray spectroscopy, reflection gratings, mono-crystalline silicon X-ray optics, electron-multiplying CCDs, suborbital rocket, grating alignment

1. INTRODUCTION

Current X-ray grating spectrometers on the *Chandra X-ray Observatory*[1] and *XMM-Newton*[2] offer modest performance ($R[\lambda/\Delta\lambda] < 1000$) in the soft X-ray bandpass ($\sim 0.3 - 2.0$ keV). However, these aging spectrometers do not have the performance necessary to answer key science questions set forth by the 2010 Astronomy and Astrophysics Decadal Survey[3] and the 2013 Astrophysics Roadmap.[4] To answer these questions, future X-ray grating spectrometers such as *Lynx*[5] require order-of-magnitude performance increases over these existing spectrometers. Technological advances in the past several decades will aid these future spectrometers in achieving the required performance increases, but many of these technologies have not yet been proven in a space environment. The Off-plane Grating Rocket Experiment (OGRE),[6,7] a soft X-ray grating spectroscopy suborbital rocket payload, provides an avenue for several of these technologies to be proven in such an environment and prepare these technologies for future large-scale X-ray spectroscopy missions such as *Lynx*.

The scientific target of the OGRE spectrometer is Capella (α Auriga), a quadruple star system composed of two binary pairs. The primary binary pair, Capella A, consists of a G8/K0 III He-burning red giant and a G1 III giant making its way through the Hertzsprung gap.[8] Strong coronal activity makes Capella A one of the brightest quiescent X-ray sources in the sky. The spectrum of Capella A is dominated by line emission, and due to its emission strength, the source is often used as a calibration target for soft X-ray spectrometers and is

Send correspondence to B.D.D.: bdonovan@psu.edu

Optics for EUV, X-Ray, and Gamma-Ray Astronomy IX, edited by Stephen L. O'Dell, Giovanni Pareschi, Proc. of SPIE
Vol. 11119, 1111911 · © 2019 SPIE · CCC code: 0277-786X/19/$21 · doi: 10.1117/12.2528858

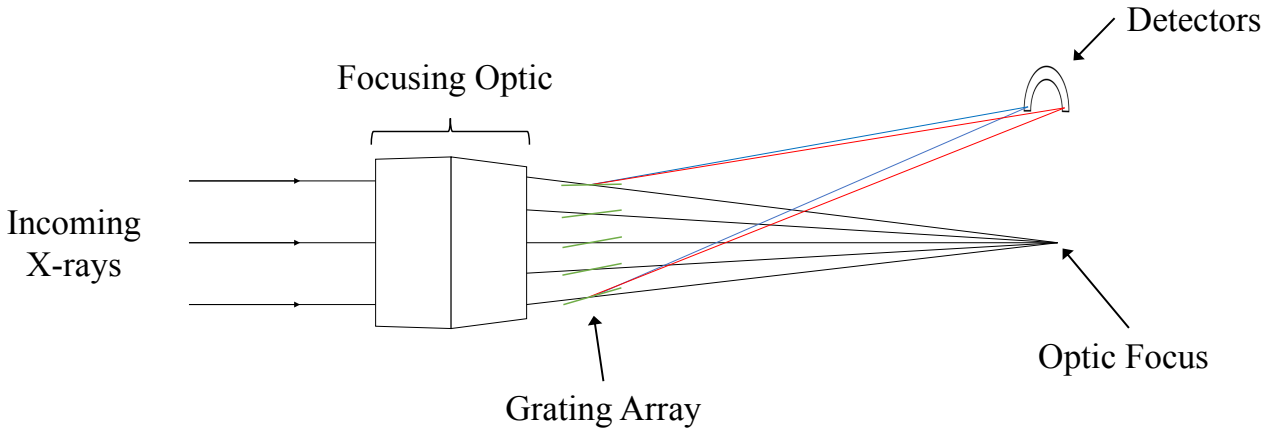

Figure 1: A schematic of the three-component X-ray spectrometer design employed on OGRE.[6] Incoming X-ray light enters from the left-hand side of the schematic and is incident on the X-ray focusing optic. The optic forms a converging X-ray beam which if left unhindered would form a focus at the optic focal plane. However, this converging light is intercepted by the grating array that diffracts this light into its component spectrum. The detectors at the spectrometer focal plane then digitize this spectrum.

included in the *Chandra* Emission Line Project.[9] These properties make it an excellent target for OGRE as the observation time of the payload is limited to ~ 300 seconds.

The OGRE spectrometer aims to achieve the highest resolution soft X-ray spectrum of Capella to date with a resolution requirement of $R > 1500$ across the entire bandpass ($\sim 10 - 55$ Å) and a goal of $R > 2000$ at select energies. This performance would surpass the spectral resolution of the Low-Energy Transmission Grating Spectrometer (LETGS)[10] and High-Energy Transmission Grating Spectrometer (HETGS)[11] on *Chandra* and the Reflection Grating Spectrometer (RGS)[12] on *XMM-Newton*. This unprecedented observation of Capella will enable existing line blends to be resolved, new and updated emission lines to be integrated into plasma spectral models to support future X-ray spectroscopy missions, and more accurate plasma characteristics for this calibration source to be determined.

To obtain this high-resolution soft X-ray spectrum of Capella, the OGRE spectrometer will utilize three key technologies: mono-crystalline silicon X-ray optics,[13] X-ray reflection gratings operated in the extreme off-plane mount,[14] and an array of electron-multiplying CCDs (EM-CCDs) at the focal plane.[15] While the suborbital rocket mission architecture provides an avenue for these three technologies to prove themselves in a space environment, the mission architecture also places unique constraints on the design of the spectrometer. An initial optical design for the soft X-ray spectrometer on OGRE is discussed in Donovan et al. (2018).[6] This manuscript will discuss an updated optical design of the OGRE soft X-ray spectrometer as well as a grating alignment concept to help realize this design.

2. OPTICAL DESIGN OF THE OGRE SOFT X-RAY SPECTROMETER

A soft X-ray spectrometer is generally composed of three components: an X-ray optic (typically a Wolter-I type[16]) that focuses the incident X-ray light, a transmission/reflection grating array that diffracts this light into its component spectrum, and an array of detectors on the focal plane that digitize the diffracted light. A schematic of this spectrometer design is shown in Figure 1. The OGRE spectrometer follows this three-component spectrometer design, with each of its components discussed below.

2.1 X-ray Optics

The OGRE spectrometer will employ a mono-crystalline silicon X-ray optic module developed by NASA Goddard Space Flight Center.[13] Each mirror segment in the optic module is produced from a block of single-crystal silicon

Table 1: The mono-crystalline silicon X-ray optic prescription for the OGRE grating spectrometer. This prescription assumes an axial mirror length of 100 mm, an axial separation of 5 mm, and a radial separation between mirrors of 1.3 mm. Shown are the optical prescriptions for each of the 12 mirror shells: the primary (paraboloid) radii at its front ($Z = 3602.5$ mm) and back ($Z = 3502.5$ mm) axial edges, the secondary (hyperboloid) radii at its front ($Z = 3498.5$ mm) and back ($Z = 3398.5$ mm) axial edges, and the radius of each shell at the intersection node of the primary and secondary mirror surfaces ($Z = 3500$ mm).

		Radius (mm)				
Mirror	**Label**	**Prim. - Front**	**Prim. - Back**	**Intersection**	**Sec. - Front**	**Sec. - Back**
1	330	166.203	165.029	165.000	164.912	161.373
2	335	168.772	167.580	167.550	167.461	163.867
3	340	171.359	170.150	170.119	170.028	166.379
4	345	173.966	172.738	172.707	172.615	168.910
5	351	176.592	175.346	175.314	175.220	171.460
6	356	179.237	177.972	177.940	177.845	174.029
			Mid-Plate			
7	388	195.523	194.143	194.108	194.004	189.841
8	394	198.308	196.908	196.873	196.767	192.545
9	399	201.113	199.693	199.658	199.551	195.269
10	405	203.938	202.499	202.463	202.355	198.013
11	411	206.785	205.326	205.289	205.179	200.777
12	416	209.653	208.173	208.136	208.025	203.561

which allows the mirrors to be manufactured free of internal stresses. Due to this stress-free nature, each mirror can achieve high angular resolution while remaining thin and light. This optic technology is the only technology that can simultaneously meet the angular resolution, effective area, and weight requirements of the OGRE spectrometer.[6] A more in-depth overview of the mono-crystalline silicon X-ray optic technology can be found in Zhang et al. (2018).[13]

The OGRE optic module will be composed of 12 shells of mono-crystalline silicon mirror segments with a shared focal length of $Z_0 = 3500$ mm and spanning radii from $r_0 = 165.000 - 208.136$ mm. The focal length of the optic module is constrained by the suborbital mission architecture to $Z = 3500$ mm – the maximum focal length allowed without compromising flight stability.

The primary and secondary mirrors for a given shell will be separated by a 5 mm axial gap with each mirror spanning an axial length of 100 mm. Each mirror will be ~ 1 mm thick with ~ 0.3 mm of additional space added between each mirror for thickness allowance. The prescription for each mirror shell in the OGRE optic module that results from the described mirror parameters is shown in Figure 1. The predicted half-power diameter performance of the optic module is < 5 arcsec. Each of the 12 shells will have 12 primary (paraboloid) and 12 secondary (hyperboloid) mirror segments for a total of 288 total mirror segments in the optic module.

2.2 X-ray Reflection Gratings

The OGRE spectrometer will employ reflection gratings operated in the extreme off-plane mount to disperse the converging light from the X-ray optic module into its component spectrum. These gratings have demonstrated both high spectral resolution and high diffraction efficiency in the soft X-ray bandpass.[17,18] These two qualities make the technology an ideal choice for OGRE since, while the spectrometer aims to obtain a high-resolution spectrum of Capella, it has only ~ 300 sec of observation time to obtain this spectrum.

Gratings in the extreme off-plane mount are oriented quasi-parallel to the groove direction and at grazing incidence relative to the incident X-ray photons as depicted in Figure 2(a). The incident X-ray photons are then dispersed conically according to the generalized grating equation:

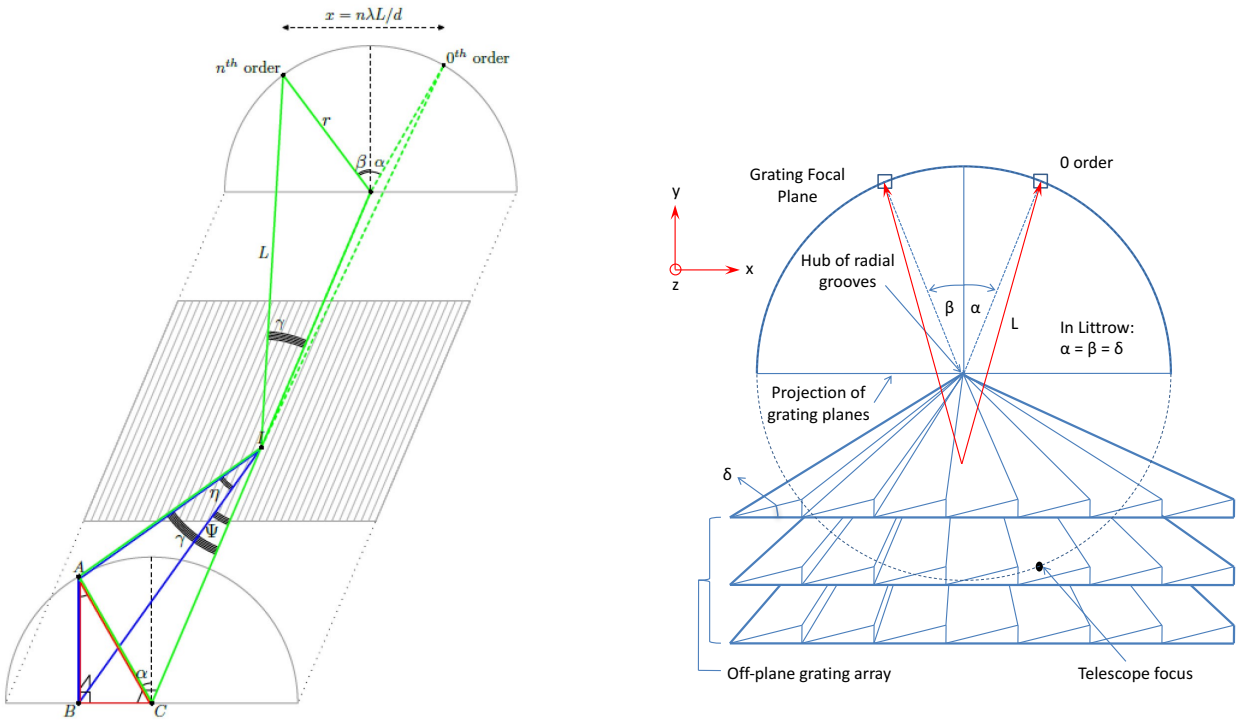

(a) (b)

Figure 2: The diffraction geometry of a reflection grating in the extreme off-plane mount.[14,17] (a): Light is incident from point A onto the grating surface at a graze angle η and relative to the groove direction by an angle Ψ. Equivalently, this incidence geometry can be described in the spherical coordinate system by azimuth angle α and polar angle γ. Diffraction follows the generalized grating equation (Eq. 1) and light is diffracted a distance L to azimuth angle β on the focal plane. The dispersion distance between the $n = 0$ reflection and n-th diffraction order on this focal plane is given by x. (b): An array of three aligned gratings whose diffraction arcs overlap at the spectrometer focal plane. The groove facets of these reflection gratings are sculpted to have a triangular (blazed) profile with facet angle δ. This groove profile serves to preferentially disperse light to the specific bandpass of interest. Maximum diffraction efficiency is realized in the Littrow mount where $\alpha = \beta = \delta$. The grooves here also have a radial profile such that all grooves converge to the center of the diffraction arc on the spectrometer focal plane. This radial profile minimizes aberrations at the focal plane, thus increasing spectral resolution. Here, the gratings are depicted to extend to the focal plane for illustrative purposes, but in reality, gratings only extend ~ 70 mm towards the focal plane.

$$\sin\alpha + \sin\beta = \frac{n\lambda}{d\sin\gamma}, \tag{1}$$

where α is the azimuthal angle of the incident light, β is the azimuthal angle of the diffracted light, γ is the polar angle of the incident light relative to the groove direction, λ is the wavelength of the light, n is the diffraction order, and d is the groove period. Differentiating this equation with respect to λ yields the dispersion relation:

$$\frac{d\lambda}{dx} = \frac{10^7}{nLD}\frac{\text{Å}}{\text{mm}}, \tag{2}$$

where L is the distance a photon travels to the spectrometer focal plane (*throw*), D is the groove density ($\equiv 1/d$), and $x = L\sin\gamma(\sin\beta+\sin\alpha)$ (*dispersion direction*). To maximize resolution, $R = \lambda/\Delta\lambda(= x/\Delta x)$, a spectrometer then must maximize dispersion and minimize the width of the line spread function (LSF) on the focal plane.

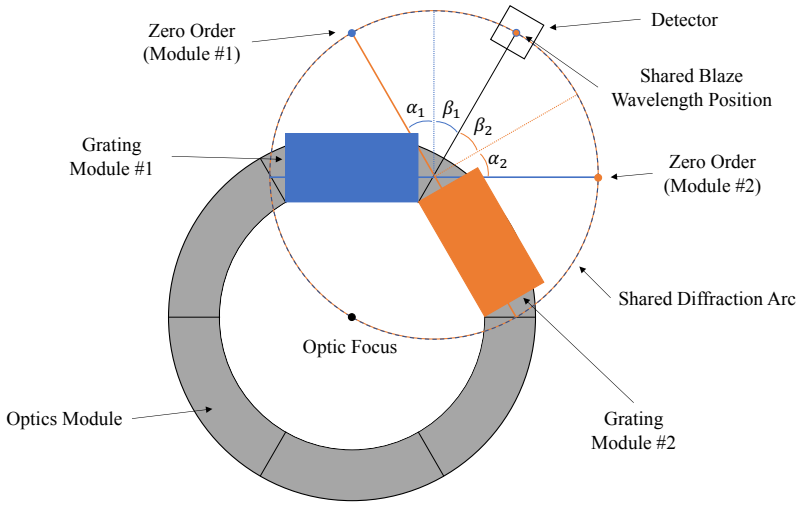

Figure 3: Diffraction geometry for the soft X-ray spectrometer on OGRE.[6] To increase the achievable spectral resolution, the optic is subapertured into six 60° azimuthal segments. Behind each of these segments is a grating module composed of 60 gratings. To maximize diffraction efficiency, each grating module operates in the Littrow mount which requires $\alpha = \beta = \delta$. Here, $\alpha = \beta = \delta = 30°$ such that neighboring 60° azimuthal segments can diffract to the same location on the focal plane. This geometry is repeated two times to populate the entire 360° azimuthal span of optic with grating modules.

Reflection gratings operating in the extreme off-plane mount typically employ grooves that radially converge to match the convergence of the X-ray optic upstream in the optical path. This groove geometry minimizes aberrations on the focal plane.[19] Furthermore, the grooves can be manufactured to have a blazed profile which preferentially diffracts the incident light to a specific bandpass of interest as seen in Figure 2(b). By manipulating the grooves in this way, reflection gratings operating in the extreme off-plane mount can simultaneously achieve high spectral resolution and high diffraction efficiency.

2.2.1 Diffraction Geometry

To increase their achievable spectral resolution, X-ray grating spectrometers can subaperture their X-ray optic such that only a portion (typically $\sim 30 - 60°$) of their full 360° azimuthal span is populated with gratings. This decreases the width of the point spread function (PSF) formed by the optic which consequently decreases the width of the LSF. By decreasing this width in the dispersion direction (Δx), the spectral resolution of the spectrometer can be improved without improving the performance of the optic. This, however, typically comes at the cost of reduced effective area.

To increase its spectral resolution while maximizing its effective area, the OGRE spectrometer will subaperture its X-ray optic module into six 60° azimuthal segments with a separate grating module behind each of these optic segments. A pair of neighboring grating modules are then oriented such that they each diffract their spectrum to the same location on the focal plane. With two grating modules diffracting to the same location, OGRE only requires three spectral detectors. A schematic of this geometry can be seen in Figure 3. The described geometry is then repeated two times to populate the entire optic with grating modules. This geometry allows OGRE to still achieve the increased resolution gained by the subaperturing technique described above, but without taking a large effective area loss generally associated with this technique. To further maximize effective area, the gratings will operate in the Littrow mount: $\alpha = \beta = \delta$, where δ is the blaze angle of the grooves. This mount realizes maximum diffraction efficiency in the extreme off-plane mount.

This grating design places constraints on the diffraction geometry of the OGRE grating modules. Since grating modules are placed behind 60° azimuthal optic segments, neighboring grating modules operating in the

Table 2: Parameters describing the diffraction geometry and grating substrates of the OGRE spectrometer.

Parameter	Value
Graze Angle (η)	1.5°
Yaw (Ψ)	±0.87°
Blaze Angle (δ)	30°
Groove Period (d; @ 3300 mm)	160 nm
Throw (L)	3251.5 mm
Grating Dimensions	∼ 70 mm x 70 mm
Grating Separation	2.182 mm
Fan Angle	2.30 arcmin

Littrow mount must have $\alpha = \beta = \delta = 30°$ to diffract to the same location on the focal plane. Additionally, the OGRE spectrometer will maximize its diffraction efficiency at the blaze wavelength:

$$n\lambda_b = 2d \sin\gamma \sin\delta. \tag{3}$$

Thus, the groove period for OGRE must be chosen to maximize the diffraction efficiency in its bandpass of interest. By constraining the graze angle to $\eta = 1.5°$ and with the grating modules placed downstream from the optic module at an axial position of $Z \approx 3250$ mm, a groove period of 160 nm is required to maximize the diffraction efficiency for the bright transition lines in the Capella spectrum between $10 - 20$ Å. This geometry gives a dispersion on the focal plane of $\sim 0.485/n$ Å/mm. A summary of the parameters for the OGRE grating geometry is shown in Table 2.

2.2.2 Grating Placement

The reflection gratings in the OGRE spectrometer will have dimensions ∼ 70 mm x 70 mm x 2.182 mm thick. To populate an entire 60° azimuthal optical segment with these gratings (∼ 150 mm wide), OGRE requires two stacks (left & right) in each grating module, each with 30 gratings stacked on top of one another. With 60 gratings per module, this requires a total of 360 gratings for the six grating modules.

The gratings in each module must be oriented such that their diffraction arcs overlap at the focal plane, which requires a fan angle of 2.30 arcmin between consecutive gratings. However, even with this fan angle, the total LSF formed by the 60 gratings in a grating module still possesses aberrations due to individual diffraction arcs not overlapping exactly. To reduce these aberrations, grating placement was numerically optimized so as to minimize induced aberrations on the focal plane.

Grating positions in the module were iterated via a numerical optimization routine to minimize the width of the LSF on the focal plane at $\lambda = 15.01$ Å. This wavelength corresponds to the Fe XVII transition line – the brightest line in the soft X-ray spectrum of Capella A. As a result of the optimization routine, the LSF aberrations induced in the dispersion direction from diffraction were effectively eliminated – the width of the LSF in the dispersion direction is actually slightly smaller than the assumed PSF width of 1.5 arcsec (= 25 µm) FWHM in the dispersion direction. With an LSF width of 22 µm FWHM, the theoretical maximum resolution at this bright Fe XVII transition line is $R = x/\Delta x \approx 4200$. An image of subapertured PSF formed by a 60° azimuthal segment of the OGRE optic module and the LSF from a single grating module is shown in Figure 4(a-b). Additionally, the optimized positions of the gratings in an OGRE grating module can be seen in Figure 4(c).

2.3 Detector Array

The detector array is the final component of the OGRE reflection grating spectrometer. As dictated by the diffraction geometry, the detector array will contain three spectral detectors observing the six spectra from the grating modules, with each of the spectral detectors observing spectra from two grating modules. While the majority of the converging beam from the optic will be intercepted by the grating modules as shown in Figure 3, a small portion of this beam will pass freely to the focal plane and form a focus. Therefore, the detector array

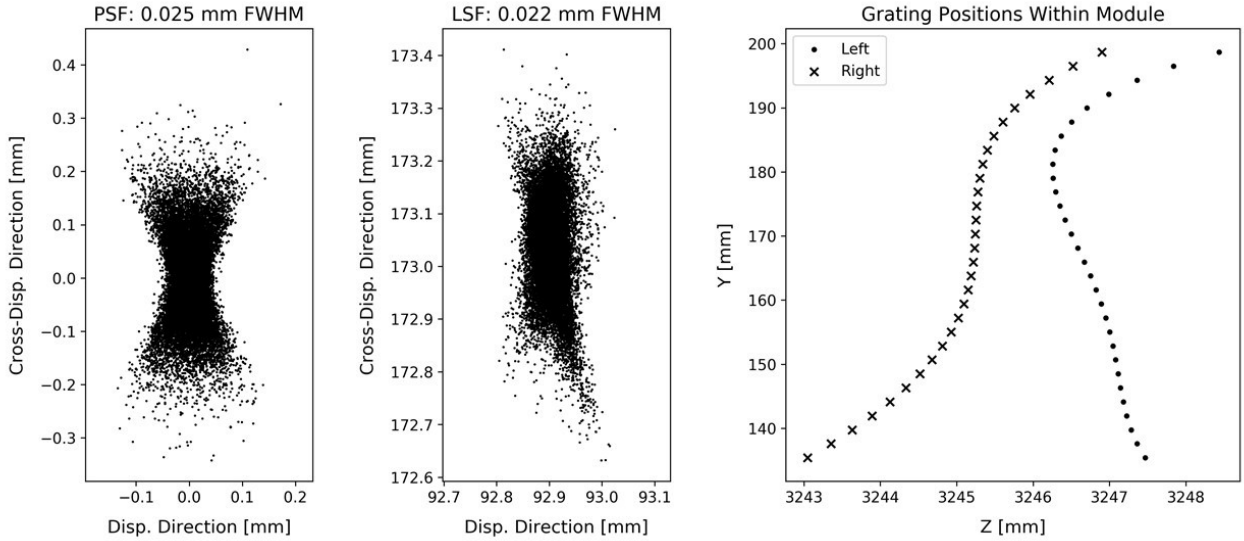

(a) (b) (c)

Figure 4: (a): The simulated point spread function (PSF) from a 60° azimuthal segment of the OGRE optic module. The simulated width is in accordance with OGRE optic performance requirements: ~ 1.5 arcsec FWHM. (b): The simulated line spread function (LSF) from a single OGRE grating module. The width of the LSF is actually slightly smaller than the PSF of the optic, likely resulting from additional subaperturing by the grating module. The resolution achieved by this simulation is $R(x/\Delta x) \approx 4200$. (c): The optimized grating positions for the left and right grating stacks used to achieve the LSF displayed in (b). Together, the left and right grating stacks form an OGRE grating module.

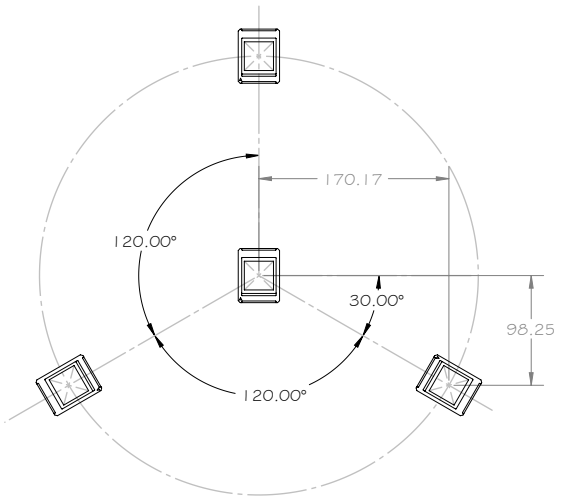

Figure 5: Focal plane layout for the soft X-ray spectrometer on OGRE in units of mm.[6] The central detector will observe the focus formed by portions of the OGRE optic module not populated with grating modules. The three outer detectors each will observe spectra from two grating modules. The spectral detectors are at axial position $Z = -3.61$ mm, while the central detector is at axial position $Z = 0$ mm.

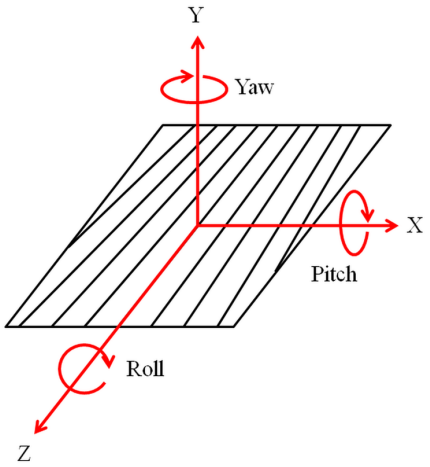

Figure 6: Degrees of freedom for a representative grating in the OGRE grating modules.[20] The spectrometer focal plane is in the $-\hat{z}$ direction.

Table 3: Tolerances for the grating-level and stack-level alignment of the OGRE grating modules. Values are from a comprehensive line spread function error budget presented in Donovan et al. (2019).[21]

Parameter	Grating-Level Tolerance [1σ level]	Stack-Level Tolerance [3σ level]
$\hat{x}$	$\pm$127 µm	$\pm$127 µm
$\hat{y}$	$\pm$127 µm	$\pm$254 µm
$\hat{z}$	$\pm$127 µm	$\pm$127 µm
Pitch (rotation about $\hat{x}$)	$\pm$30 arcsec	$\pm$60 arcsec
Yaw (rotation about $\hat{y}$)	$\pm$30 arcsec	$\pm$60 arcsec
Roll (rotation about $\hat{z}$)	$\pm$15 arcsec	$\pm$30 arcsec

will also contain a fourth detector to observe the focus formed by the light from the OGRE optic module that is not intercepted by the six grating modules.

The four detectors must be placed to minimize the path length differences from either photons diffracting from individual gratings in the OGRE grating modules or from photons reflecting from the optic module. In the case of the central optic focus detector, the location where the path length differences are minimized will achieve maximum angular resolution. This location is dictated by the focal length of the optic module: 3500 mm. With the optic module at an axial position of $Z = 3500$ mm, this requires that the central detector is at an axial position of $Z = 0$ mm.

Similarly, the location where the path length differences are minimized for the spectral detectors will achieve maximum spectral resolution. The grating modules for OGRE are yawed with respect to the converging light from the optic module. To minimize aberrations for a single grating module, an angle focal plane is required. However, since each detector will monitor two spectra simultaneously, each spectral detector must be placed to simultaneously minimize aberrations from both of its grating modules. This requires a flat focal plane which bisects the optimal focal planes of the two grating modules it observes. The axial position of each spectral detector is $Z = -3.61$ mm and each is centered about the centroid of the blaze wavelength: $n\lambda_b = 47.6$ Å. A schematic showing the relative placement of the four detectors on the focal plane is shown in Figure 5.

3. A NEW GRATING ALIGNMENT CONCEPT

The comprehensive LSF error budget for the OGRE spectrometer[21] identifies contributors to the final LSF observed by the spectrometer including alignment tolerances required for grating-to-grating and stack-to-stack misalignments. A summary of these alignment tolerances is shown in Table 3. Gratings must be aligned to these tolerances to enable the spectrometer to realize its optical design.

3.1 Previous Grating Alignment Methodology

To attain grating alignment tolerances in the past, reflection grating spectrometers employed an active approach to grating alignment wherein each grating within a module is actively aligned with a hexapod or similar staging.[22] After each grating is maneuvered into alignment, it is then fixed into place with epoxy. This process continues until all gratings have been populated into the module. This method was employed for the Water Recovery X-ray Rocket (WRXR)[22] and was studied for the reflection grating spectrometer concept for *Arcus*.[20] While practical for missions that require a small amount of gratings (< 30) such as WRXR, this method quickly becomes impractical for missions requiring a large amount of gratings such as OGRE. For example, the alignment of the 26 gratings required for the WRXR grating module took on the order of two weeks. Extrapolating this rate to the OGRE spectrometer which requires 360 gratings, a similar active grating alignment methodology might take on the order of 27 weeks to complete.

The limiting factor of the active grating alignment methodology employed for the WRXR grating module was the epoxy used to bond each grating into the module. The work time of the epoxy meant that aligning more than two gratings per day with a single alignment station was not feasible. Furthermore, this alignment effort saw grating orientation shifts of $\sim 5-15$ arcsec during the first several hours of the epoxy cure. These shifts are on the order of OGRE grating-level alignment tolerances. Thus, a new method of grating alignment that is not prone to these epoxy-related issues was desired.

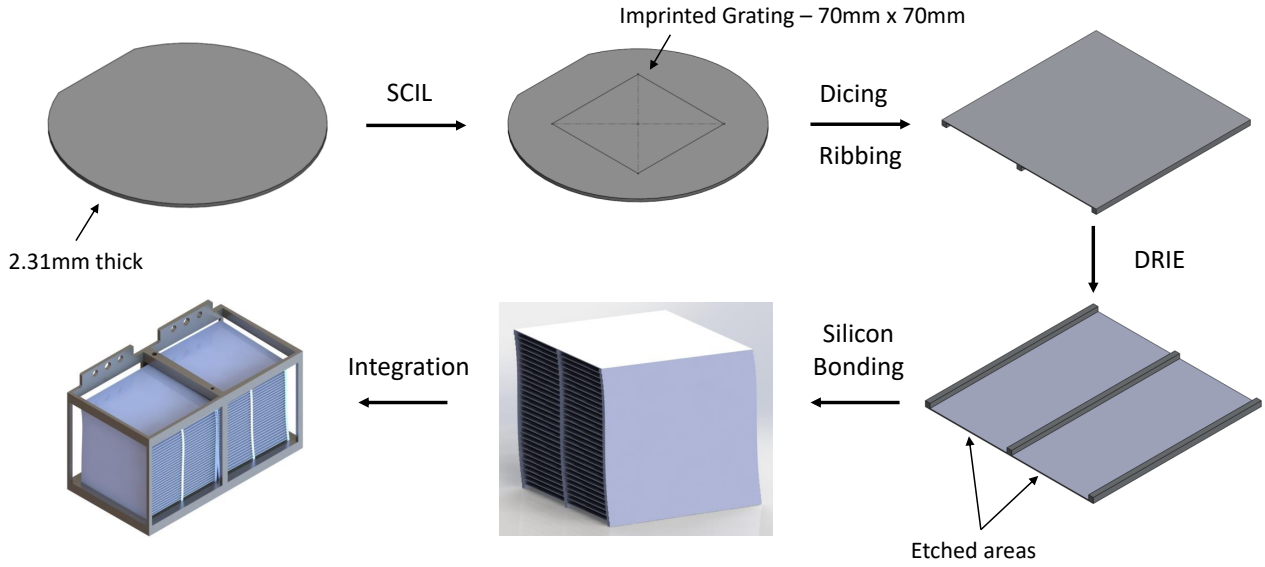

Figure 7: An overview of the proposed grating alignment methodology for the OGRE grating modules. The procedure starts by procuring precision wedged grating substrates from optic manufacturers that meet the desired tolerances shown in Table 3 (top-left). Then, a grating is imprinted on the top surface of this wedged substrate via substrate conformal imprint lithography (top-center). The grating substrate is then diced into a rectangular shape and the backside of the substrate is "ribbed" such that only three 2mm wide ribs remain (top-right). The back surface is then etched via deep reactive ion etching to remove the topmost substrate layer containing an surface irregularities which might cause unwanted stress (bottom-right). The grating substrates are then stacked on top of one another and bonded together via direct bonding to form a grating stack (bottom-center). Two of these grating stacks are then aligned together into one of six OGRE grating modules (bottom-left).

3.2 A Proposed Alignment Methodology for OGRE

A method not prone to the previous epoxy-related issues has been devised for implementation on OGRE and is based upon the silicon pore optic (SPO) technology developed by cosine Research B.V.[23] Instead of actively aligning each grating individually with a hexapod as in the past, this alignment method relies on a more passive approach wherein much of the alignment is manufactured into the grating substrates themselves. With substrates that meet the tolerances in Table 3, simply stacking the substrates with a precision robot will ensure that the alignment tolerances can be met. Furthermore, the substrates will be bonded together via direct bonding,[24] a chemical process that does not rely on external adhesive, thereby eliminating epoxy from the grating alignment process.

A detailed description of the envisioned process is described in the following paragraphs and is outlined in Figure 7. The process begins with the manufacture of the grating substrates themselves. These grating substrates will be manufactured on fused silica or silicon and procured from specialty optic manufacturers. The substrates are manufactured such that their thickness and wedge angle reflect the designed separation and fan angle between consecutive gratings. Grating-to-grating alignment tolerances in pitch, roll, and $\hat{y}$ then fall largely on the manufacturing tolerances of the wedged substrates.

Once the wedged substrates have been procured, the gratings are then imprinted onto the top surface via substrate conformal imprint lithography (SCIL).[25] This process was used to fabricate the flight gratings for the WRXR.[26,27] During wedge manufacture, the high side of the wedge is aligned to the wafer flat which is then referenced during the initial imprint alignment. Simulations show that this alignment is not critical and can have errors on the order of $\sim 1 - 2°$.

Once imprinted, the grating is then coated with a photoresist to protect the grating pattern from subsequent processing steps. The grating is then diced into a rectangle and ribs are cut into the backside of the grating substrate. This process references alignment markers imprinted with the grating pattern such that the rectangle and ribs are aligned within $\sim 1-2$ µm of the grating pattern. The ribbing process allows the precise tolerances in pitch (rotation about $\hat{x}$), roll (rotation about $\hat{z}$), and $\hat{y}$ initially manufactured into the substrates to be maintained, while giving light a path to diffract from the grating surface. However, this ribbing and dicing process induces stress into the grating substrate which distorts the grating surface out of specification for both pitch and roll.

To relieve this induced stress, the back surface of the grating is etched approximately $\sim 20-80$ µm via deep reactive ion etching (DRIE). This process removes damaged surface layers caused by the ribbing process and restores the grating surface back to its pre-ribbed figure. To prevent damaging the pristine top surfaces of the ribs during this process, a protective photoresist is applied prior to etching. Once ribbed, diced, and etched, the photoresist protecting the grating pattern and the tops of the ribs is removed.

A unique property of the sol-gel resist variant used for this particular SCIL process is that it is silica-based (Phillips SCIL Nanoimprint Solutions) and it becomes 100% fused silica when annealed.[28] Therefore, the same chemistry that enables silicon and fused silica direct bonding enables sol-gel direct bonding to either fused silica or silicon. With the substrates prepared for direct bonding, the grating substrates are then stacked on top of one another using a precision robot similar to the SPO alignment process.[23] These robots have been developed and extensively tested for SPO mirror module production and can achieve the alignment tolerances in $\hat{x}$, $\hat{z}$, and yaw (rotation about $\hat{y}$). Once fully stacked, the grating stacks are annealed to improve the strength of the direct bonds.

Once both stacks are produced for a given grating module, the stacks will be aligned to one another and integrated into a grating module. An in-depth discussion of stack and module integration is given in O'Meara et al. (2019).[29]

This new reflection grating alignment concept is anticipated to be much improved over previous grating alignment methods. The difficulty of alignment now falls largely on grating substrate production which utilizes proven optical manufacturing and nano-fabrication processes. Furthermore, if similar stacking times to those that have been achieved for SPO module alignment (< 1 h),[23] the alignment of all 360 gratings into grating stacks will take $\sim 1-2$ months instead of the > 6 months as would have been the case for the previous alignment methodology.

4. CURRENT PROGRESS & FUTURE WORK

A great deal of progress has been made on the OGRE spectrometer in the past year. In the following section, a status update will be given for each major component of the spectrometer (optic module, grating modules, detector array) and future plans for each will be discussed.

4.1 Optic Module

A more in-depth discussion of recent results and future work for the mono-crystalline silicon optic technology can be found in Zhang et al. (2018),[13] but a summary of this discussion as it relates to OGRE will be discussed here. Prototype single-shell OGRE optics have entered production. An image of one of these prototypes can be seen in Figure 8(a). An optic prototype will be produced in the early fall of 2019, after which the optic will be tested for performance in the 47 m X-ray beamline at Penn State. This facility has been used in the past for lobster-eye testing and detector characterization.[30] Once performance is verified, focus will switch to the production of a 2-3 shell prototype optic stack. The performance of this optic is expected to be verified at the Max Planck Institute for Extraterrestrial Physics' PANTER X-ray Test Facility in Neuried, Germany. This facility has extensive experience testing X-ray optics for *Athena*,[31] *Arcus*,[32] and for previous mono-crystalline silicon optic testing.[13] Once the performance of this multi-shell optic prototype is verified, production will begin on the flight OGRE optic assembly.

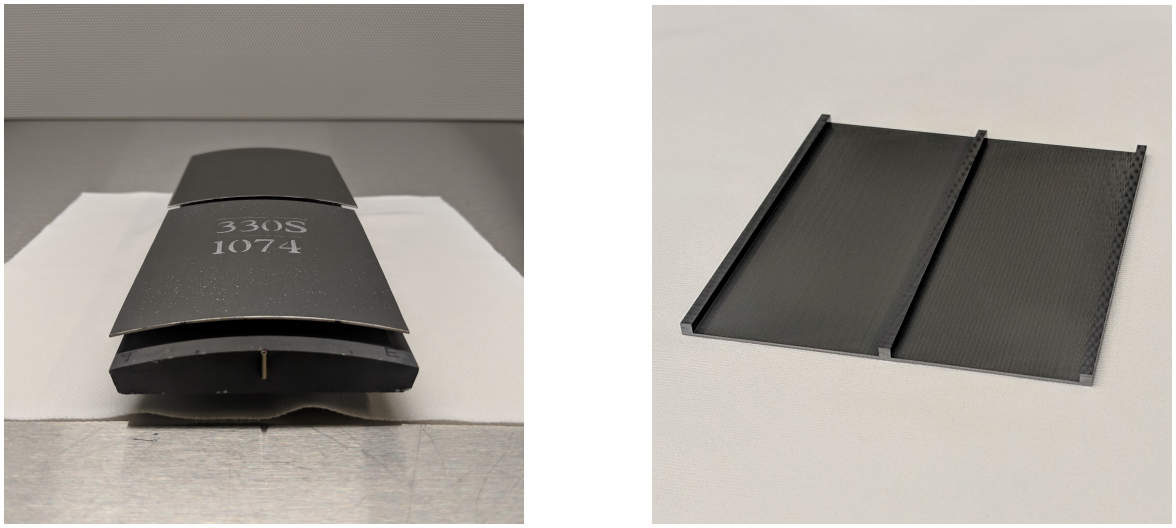

(a) (b)

Figure 8: Single-shell optic (a) and grating substrate (b) prototypes for the OGRE spectrometer.

4.2 Grating Modules

All aspects of grating production, alignment, and integration are currently in development. Grating master prototypes have been manufactured via electron-beam lithography in the Nanofabrication Laboratory at Penn State and tested for performance at the PANTER X-ray Test Facility in Neuried, Germany. Preliminary results indicate that one of these gratings meets the performance requirement for OGRE, and concluding results from this test are forthcoming.[33] Regarding grating replication development, prototype SCIL grating replicas have been procured from Moxtek, Inc. These prototype replicas will be tested for performance in the 47 m Penn State beamline with an OGRE optic prototype in early fall of 2019. Additionally, SCIL tooling has been recently procured and commissioned by the Nanofabrication Laboratory at Penn State, which will greatly aid in future SCIL process development.

In addition to grating fabrication and replication development, grating alignment process development has commenced. Initial silicon grating prototypes have been procured from several optic manufacturers and these vendors are currently iterating on their production processes to meet the required specifications. Fused silica substrates are also being procured. The ribbing of these substrates is also well underway and the first several batches of ribbed substrates have been delivered. An example of a ribbed substrate can be seen in Figure 8(b). Initial processing runs have shown that this ribbing process induces large amounts of stress into the substrate. This stress distorts the figure of the grating substrates such that they no longer meet the alignment tolerances as described in Table 3. Initial stress mitigation studies with DRIE show that this induced stress can be alleviated though with the etched gratings returning to their pre-ribbed figure.

Direct bonding has also been successfully demonstrated by cosine Research B.V. During this direct bonding study, two variations of direct bonding were studied: silicon–silicon and silicon–sol-gel. Silicon–sol-gel bonding is an important process to test since this silica-based sol-gel resist will coat the entire top surface of the grating after SCIL replication. Work has now shifted towards showing that fused silica can bond to sol-gel. Direct bonding has also been recently demonstrated at Penn State.

The culmination of these development efforts is the production of a prototype stack consisting of $2-3$ gratings that will be tested with the $2-3$ shell OGRE optic prototype at the PANTER X-ray Test Facility before the end of 2019. If successful, this test will prove alignment methodologies for both the OGRE mirror module and the OGRE grating stacks. Efforts then would be shifted towards producing the flight OGRE grating stacks.

4.3 Detector Array

Prototype detectors for the OGRE payload have been extensively characterized.[15] Furthermore, a final design of the flight OGRE detector assembly has been completed by XCAM Ltd. A comprehensive design review has taken place and work has begun sourcing mechanical components for the assembly. The detector assembly will continue production for the next several months with completion slated for early 2020. After the detector assembly has been manufactured, The Open University will take delivery of the detector assembly for testing and characterization. Penn State will then take delivery of this assembly in mid-2020.

5. SUMMARY

In this manuscript, an optical design for the soft X-ray grating spectrometer on the Off-plane Grating Rocket Experiment (OGRE) was described. This design will allow the OGRE spectrometer to obtain the highest resolution soft X-ray spectrum of an astronomical source to date. Furthermore, a new grating alignment concept based on the silicon pore optic (SPO) technology has been outlined. This concept aims to improve upon the shortcomings of a previous grating alignment methodology used to align the Water Recovery X-ray Rocket grating module. Finally, recent progress on the OGRE payload was described and a outline of milestones in the near future were discussed.

ACKNOWLEDGMENTS

The work presented here is supported by NASA grant NNX17AD19G, a NASA Space Technology Research Fellowship, and internal funding from The Pennsylvania State University.. The authors would like to thank the staff members of the Nanofabrication Laboratory at Penn State's Materials Research Institute, and current and past members of the McEntaffer research group for their support of this project. This work makes use of PyXFocus, an open-source Python-based raytrace package.

REFERENCES

[1] Weisskopf, M. C., "Astronomy and astrophysics with the Advanced X-ray Astrophysics Facility," *Space Science Reviews* **47**, 47–93 (Mar 1988).

[2] Jansen, F., Lumb, D., Altieri, B., Clavel, J., Ehle, M., Erd, C., Gabriel, C., Guainazzi, M., Gondoin, P., Much, R., Munoz, R., Santos, M., Schartel, N., Texier, D., and Vacanti, G., "XMM-Newton Observatory - I. The Spacecraft and Operations," *A&A* **365**(1), L1–L6 (2001).

[3] Council, N. R., [*New Worlds, New Horizons in Astronomy and Astrophysics*], The National Academies Press, Washington, DC (2010).

[4] Kouveliotou, C., Agol, E., Batalha, N., Bean, J., Bentz, M., Cornish, N., Dressler, A., Figueroa-Feliciano, E., Gaudi, S., Guyon, O., Hartmann, D., Kalirai, J., Niemack, M., Ozel, F., Reynolds, C., Roberge, A., Straughn, K. S. A., Weinberg, D., and Zmuidzinas, J., "Enduring Quests-Daring Visions (NASA Astrophysics in the Next Three Decades)," *ArXiv e-prints* (Jan. 2014).

[5] Gaskin, J. A., Allured, R., Bandler, S. R., Basso, S., Bautz, M. W., Baysinger, M. F., Biskach, M. P., Boswell, T. M., Capizzo, P. D., Chan, K.-W., Civitani, M. M., Cohen, L. M., Cotroneo, V., Davis, J. M., DeRoo, C. T., DiPirro, M. J., Dominguez, A., Fabisinski, L. L., Falcone, A. D., Figueroa-Feliciano, E., Garcia, J. C., Gelmis, K. E., Heilmann, R. K., Hopkins, R. C., Jackson, T., Kilaru, K., Kraft, R. P., Liu, T., McClelland, R. S., McEntaffer, R. L., McCarley, K. S., Mulqueen, J. A., Özel, F., Pareschi, G., Reid, P. B., Riveros, R. E., Rodriguez, M. A., Rowe, J. W., Saha, T. T., Schattenburg, M. L., Schnell, A. R., Schwartz, D. A., Solly, P. M., Suggs, R. M., Sutherlin, S. G., Swartz, D. A., Trolier-McKinstry, S., Tutt, J. H., Vikhlinin, A., Walker, J., Yoon, W., and Zhang, W. W., "Lynx Mission concept status," *Proc. SPIE* **10397**, 103970S (2017).

[6] Donovan, B. D., McEntaffer, R. L., Tutt, J. H., Schultz, T. B., Biskach, M. P., Chan, K.-W., Hlinka, M., Kearney, J. D., Mazzarella, J. R., McClelland, R. S., Riveros, R. E., Saha, T. T., Zhang, W. W., Holland, A. D., Lewis, M. R., Soman, M. R., Holland, K., and Murray, N. J., "Optical design of the Off-plane Grating Rocket Experiment," **10699**, 106993U (2018).

[7] Tutt, J. H., McEntaffer, R. L., Donovan, B., Schultz, T. B., Biskach, M. P., Chan, K.-W., Kearney, J. D., Mazzarella, J. R., McClelland , R. S., Riveros, R. E., Saha, T. T., Hlinka, M., Zhang, W. W., Soman, M. R., Holland, A. D., Lewis, M. R., Holland, K., and Murray, N. J., "The Off-plane Grating Rocket Experiment (OGRE) system overview," *Proc. SPIE* **10699**, 106996H (2018).

[8] Johnson, O., Drake, J. J., Kashyap, V., Brickhouse, N. S., Dupree, A. K., Freeman, P., Young, P. R., and Kriss, G. A., "The Capella Giants and Coronal Evolution across the Hertzsprung Gap," *ApJ* **565**(2), L97–L100 (2002).

[9] Brickhouse, N. S., "Atomic data in X-ray Astrophysics: The Chandra Emission Line Project," in [*Atomic and Molecular Data and their Applications, ICAMDATA*], Berrington, K. A. and Bell, K. L., eds., *American Institute of Physics Conference Series* **543**, 142–154 (2000).

[10] Brinkman, A. C., Gunsing, C. J. T., Kaastra, J. S., van der Meer, R. L. J., Mewe, R., Paerels, F., Raassen, A. J. J., van Rooijen, J. J., Bräuninger, H., Burkert, W., Burwitz, V., Hartner, G., Predehl, P., Ness, J. U., Schmitt, J. H. M. M., Drake, J. J., Johnson, O., Juda, M., Kashyap, V., Murray, S. S., Pease, D., Ratzlaff, P., and Wargelin, B. J., "First Light Measurements of Capella with the Low-Energy Transmission Grating Spectrometer aboard the Chandra X-Ray Observatory," *ApJ* **530**(2), L111–L114 (2000).

[11] Canizares, C. R., Huenemoerder, D. P., Davis, D. S., Dewey, D., Flanagan, K. A., Houck, J., Markert, T. H., Marshall, H. L., Schattenburg, M. L., Schulz, N. S., Wise, M., Drake, J. J., and Brickhouse, N. S., "High-Resolution X-Ray Spectra of Capella: Initial Results from the Chandra High-Energy Transmission Grating Spectrometer," *ApJ* **539**(1), L41–L44 (2000).

[12] den Herder, J. W., Brinkman, A. C., Kahn, S. M., Brand uardi-Raymont, G., Thomsen, K., Aarts, H., Audard, M., Bixler, J. V., den Boggende, A. J., Cottam, J., Decker, T., Dubbeldam, L., Erd, C., Goulooze, H., Güdel, M., Guttridge, P., Hailey, C. J., Janabi, K. A., Kaastra, J. S., de Korte, P. A. J., van Leeuwen, B. J., Mauche, C., McCalden, A. J., Mewe, R., Naber, A., Paerels, F. B., Peterson, J. R., Rasmussen, A. P., Rees, K., Sakelliou, I., Sako, M., Spodek, J., Stern, M., Tamura, T., Tandy, J., de Vries, C. P., Welch, S., and Zehnder, A., "The Reflection Grating Spectrometer on board XMM-Newton," *A&A* **365**, L7–L17 (2001).

[13] Zhang, W. W., Allgood, K. D., Biskach, M. P., Chan, K.-W., Hlinka, M., Kearney, J. D., Mazzarella, J. R., McClelland, R. S., Numata, A., Riveros, R. E., Saha, T. T., and Solly, P. M., "Astronomical x-ray optics using mono-crystalline silicon: high resolution, light weight, and low cost," *Proc. SPIE* **10699**, 106990O (2018).

[14] McEntaffer, R., DeRoo, C., Schultz, T., Gantner, B., Tutt, J., Holland, A., O'Dell, S., Gaskin, J., Kolodziejczak, J., Zhang, W. W., Chan, K., Biskach, M., McClelland, R., Iazikov, D., Wang, X., and Koecher, L., "First results from a next-generation off-plane X-ray diffraction grating," *Experimental Astronomy* **36**, 389–405 (Aug 2013).

[15] Lewis, M. R. F., Soman, M. R., Holland, A. D., Murray, N. J., Hall, D., Weatherill, D. P., Tutt, J. H., McEntaffer, R. L., DeRoo, C. T., Schultz, T. B., and Holland, K., "Development of the x-ray camera for the OGRE sub-orbital rocket," *Proc. SPIE* **9915**, 991506 (2016).

[16] Wolter, H., "Spiegelsysteme streifenden einfalls als abbildende optiken für röntgenstrahlen," *Ann. Phys.* **445**(1-2), 94–114 (1952).

[17] Miles, D. M., McCoy, J. A., McEntaffer, R. L., Eichfeld, C. M., Lavallee, G., Labella, M., Drawl, W., Liu, B., DeRoo, C. T., and Steiner, T., "Fabrication and Diffraction Efficiency of a Large-format, Replicated X-Ray Reflection Grating," *ApJ* **869**(2), 95 (2018).

[18] DeRoo, C. T., "X-ray Reflection Gratings Operated in an Echelle Mount," *Applied Optics* (In Prep).

[19] Cash, W. C., "X-ray spectrographs using radial groove gratings," *Appl. Opt.* **22**, 3971–3976 (Dec 1983).

[20] Allured, R., Donovan, B. D., DeRoo, C. T., Marlowe, H. R., McEntaffer, R. L., Tutt, J. H., Cheimets, P. N., Hertz, E., Smith, R. K., Burwitz, V., Hartner, G., and Menz, B., "Optical and X-ray alignment approaches for off-plane reflection gratings," *Proc. SPIE* **9603**, 960315 (Sept. 2015).

[21] Donovan, Benjamin D. McEntaffer, R. L., Tutt, J. H., O'Meara, B. C., Grisé, F., Allgood, K. D., Biskach, M. P., Chan, K.-W., Hlinka, M., Kearney, J. D., Mazzarella, J. R., McClelland, R. S., Numata, A., Riveros, R. E., Saha, T. T., Solly, P. M., Zhang, W. W., Holland, A. D., Lewis, M. R., Soman, M. R., and Holland, K., "A comprehensive line spread function error budget for the Off-plane Grating Rocket Experiment," *in these proceedings* .

[22] Tutt, J. H., McEntaffer, R. L., Miles, D. M., Donovan, B. D., and Hillman, C., "Grating Alignment for the Water Recovery X-Ray Rocket (WRXR)," *Journal of Astronomical Instrumentation* **8**(2), 1950009 (2019).

[23] Collon, M. J., Vacanti, G., Barriere, N., Landgraf, B., Guenther, R., Vervest, M., van der Hoeven, R., Chatbi, A., Girou, D., Sforzini, J., Beijersbergen, M. W., Bavdaz, M., Wille, E., Fransen, S., Shortt, B., Haneveld, J., Booysen, K., Koelewijn, A., Wijnperlé, M., van Baren, C., Eigenraam, A. e., Müller, P., Krumrey, M., Burwitz, V., Spiga, D., Pareschi, G., Massahi, S., Christensen, F., Della Monica Ferreira, D., Valsecchi, G., Oliver, P., Chequer, I., Ball, K., and Zuknik, K.-H., "Silicon pore optics mirror module production and testing," *Proc. SPIE* **10699**, 106990Y (2018).

[24] Moriceau, H., Rieutord, F., Fournel, F., Tiec, Y. L., Cioccio, L. D., Morales, C., Charvet, A. M., and Deguet, C., "Overview of recent direct wafer bonding advances and applications," *Advances in Natural Sciences: Nanoscience and Nanotechnology* **1**, 043004 (feb 2011).

[25] Verschuuren, M. A., Megens, M., Ni, Y., van Sprang, H., and Polman, A., "Large area nanoimprint by substrate conformal imprint lithography (SCIL)," *Advanced Optical Technologies* **6**, 243–264 (2017).

[26] Verschuuren, M. A., McCoy, J., Huber, R. P., van Brakel, R., Paans, M., and Voorkamp, R., "AutoSCIL 200mm tooling in production, x-ray optics, and cell growth templates," *Proc. SPIE* **10584**, 105840Z (2018).

[27] Miles, D. M., Hull, S. V., Schultz, T. B., Tutt, J. H., Wages, M., Donovan, B. D., McEntaffer, R. L., Falcone, A. D., Anderson, T., Bray, E., Burrows, D. N., Chattopadhyay, T., Eichfeld, C. M., Empson, N., Grisé, F., Hillman, C. R., McCoy, J. A., McQuaide, M., Myers, B. J., Steiner, T., Verschurren, M. A., Yastishock, D., and Zhang, N., "The Water Recovery X-ray Rocket grating spectrometer," *JATIS* (Accepted).

[28] Verschuuren, M. A., *Substrate Conformal Imprint Lithography for Nanophotonics*, PhD Dissertation, Utrecht University (2010).

[29] O'Meara, B. C., Donovan, B. D., Tutt, James H.and McEntaffer, R. L., Schultz, T. B., Allgood, K. D., Biskach, M. P., Chan, K.-W., Hlinka, M., Kearney, J. D., Mazzarella, J. R., McClelland, R. S., Numata, A., Riveros, R. E., Saha, T. T., Solly, P. M., Zhang, W. W., Holland, A. D., Lewis, M. R., Soman, M. R., and Holland, K., "The opto-mechanical design for the Off-plane Grating Rocket Experiment," *in these proceedings* .

[30] Chattopadhyay, T., Falcone, A., Burrows, D. N., Bray, E., McQuaide, M., Kern, M., Wages, M., Hull, S., Inneman, A., Hudec, R., and Stehlikova, V., "Characterization of X-ray Lobster Optics with a Hybrid CMOS sensor," in [*American Astronomical Society Meeting Abstracts #231*], *American Astronomical Society Meeting Abstracts* **231**, 355.35 (2018).

[31] Nandra, K., "Athena: Exploring the Hot and Energetic Universe," in [*AAS/High Energy Astrophysics Division #14*], *AAS/High Energy Astrophysics Division*, 301.01 (Aug 2014).

[32] Smith, R. K., Abraham, M., Allured, R., Bautz, M., Bookbinder, J., Bregman, J., Brenneman, L., Brickhouse, N. S., Burrows, D., Burwitz, V., Cheimets, P. N., Costantini, E., Dawson, S., DeRoo, C., Falcone, A., Foster, A. R., Gallo, L., Grant, C. E., Günther, H. M., Heilmann, R. K., Hertz, E., Hine, B., Huenemoerder, D., Kaastra, J. S., Kreykenbohm, I., Madsen, K. K., McEntaffer, R., Miller, E., Miller, J., Morse, E., Mushotzky, R., Nandra, K., Nowak, M., Paerels, F., Petre, R., Poppenhaeger, K., Ptak, A., Reid, P., Sanders, J., Schattenburg, M., Schulz, N., Smale, A., Temi, P., Valencic, L., Walker, S., Willingale, R., Wilms, J., and Wolk, S. J., "Arcus: exploring the formation and evolution of clusters, galaxies, and stars," *Proc. SPIE* **10397**, 103970Q (2017).

[33] Donovan, B. D., "Performance Testing of X-Ray Reflection Gratings Produced via Electron-Beam Lithography," *Applied Optics* (In Prep).